How self-assembled nanodomains can impact the organization of a phospholipid monolayer - Flower-like arrays

Osamu Shibata, Marie Pierre Krafft, Hiromichi Nakahara

How self-assembled nanodomains can impact the organization of a phospholipid monolayer - Flower-like arrays

Hiromichi Nakahara,[c] Marie Pierre Krafft,*[b] and Osamu Shibata *[a]

[a] Prof. O. Shibata
Department of Biophysical Chemistry
Nagasaki International University
2825-7 Huis Ten Bosch, Sasebo, Nagasaki 859-3298, Japan
E-mail: wosamu@niu.ac.jp
[b] Dr. M.P. Krafft
Institut Charles Sadron (CNRS)
University of Strasbourg
67034 Strasbourg, France
E-mail: marie-pierre.krafft@ics-cnrs.unistra.fr
[b] Dr. H. Nakahara
Department of Industrial Pharmacy
Daiichi University of Pharmacy
22-1 Tamagawa-cho, Minami-ku Fukuoka 815-8511, Japan

Supporting information for this article is given via a link at the end of the document.

Abstract: We found that monolayers of dipalmitoylphosphatidylcholine (DPPC) and semi-fluorinated tetrablock di(*F10H16*) self-assemble to form a new type of large, complex flower-like patterns on the surface of water and on solid substrates. The hierarchical organization of these unusual self-assemblies was investigated using compression and surface potential isotherms, *in situ* fluorescence and Brewster angle microscopies, and atomic force microscopy after transfer.

Two-dimensional mesoscopic structural patterns such as striped and circular domains are known to form spontaneously in various systems, including nanoparticles,[1] block copolymers[2] and surfactants[3]. Domain shapes and shape transitions have intensively been investigated in phospholipid films, as they pertain to the self-assembling process of microdomains in plasma membranes, such as functional rafts.[4] The characteristic length scale of the patterns is set by the balance between attractive interactions among the molecules, or objects, and the line tension that minimizes the domain boundary, hence its size.[5] The purpose of this study is to determine the changes imparted to a interfacial phospholipid film structure and behavior by co-dispersing the lipid with a powerfully self-assembling, regular nanopattern-generating molecule, and to characterize the resulting hierarchical organization. Semi-fluorinated alkane diblocks ($C_nF_{2n+1}C_mH_{2m+1}$, *FnHm*) or tetrablocks (di(*FnHm*), Figure 1a), which combine hydrocarbon and fluorocarbon segments, generate quasi-crystalline arrays of monodisperse circular nanoscopic surface domains on liquid and solid substrates.[6] These nanodomains (diameter 30–50 nm, one molecule thick) self-assemble spontaneously on water even at zero surface pressure and display elastic 2D gels properties.[7] The cohesion between *FnHm* molecules within domains results from van der Waals attractions, while the repulsion forces that prevent their coalescence originate from the dipoles of the terminal CF_3 group and CF_2-CH_2 junction.

Binary systems involving phospholipids, surfactants or polymers, and *FnHm* diblocks or related compounds have been studied.[3, 8] The general view is that the nanodomains coexist with the phospholipid monolayer without disturbing it. At high surface pressure, the nanodomains were found to glide onto the phospholipid monolayers while maintaining a vertical phase separation.[9] *FnHm* diblocks have diverse applications in medicine, e.g. ophthalmology,[10] intravascular oxygen delivery,[11]

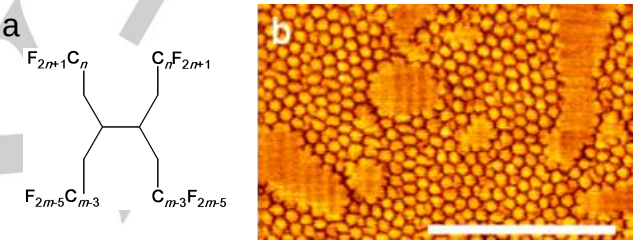

Figure 1. a) Molecular structure of semi-fluorinated tetrablocks di(*FnHm*) *n* = 8 or 10, and *m* = 16, 18 or 20; b) Atomic force microscopy (AFM) topographic image of a monolayer of di(*F*10*H*16) transferred at 5 mN m^{-1} onto mica showing a close-packed layer of nanodomains (~40 nm in diameter, which corresponds to the length of the fully expanded di(*F*10*H*16) molecule (3.7 nm). The scale bar represents 500 nm.

diagnosis,[12] and biomedical research.[13] They also proved effective for stabilizing and reducing the permeability of liposomes and, more generally, for controlling phospholipid self-assembly and film properties[14] In some applications, *FnHm* diblocks are in contact, and likely interact with phospholipids of cell membranes. However, reports on interactions between phospholipids and fluorocarbons remain scarce. Some papers have reported the miscibility of phospholipid monolayers with perfluoroalkylated acids.[15]

Here, we study the perturbations caused by nanodomains of semi-fluorinated tetrablock di(*F*10*H*16) and a dipalmitoylphosphatidylcholine (DPPC) Langmuir monolayer. Langmuir monolayers of di(*F*10*H*16) consist of nanodomains (40 nm in diameter, Figure 1b)). The tetrablock was selected because the patterned films it forms are particularly sturdy,[16] and DPPC because of its prominence in the lung surfactant[17] and its conveniently positioned liquid expanded (LE)/liquid condensed (LC) phase transition. We actually discovered a totally new type of 2D organization in the mixed DPPC/di(*F*10*H*16) monolayers.

The mixed monolayers formed by co-spreading DPPC and di(*F*10*H*16) on water in a Langmuir trough were investigated by

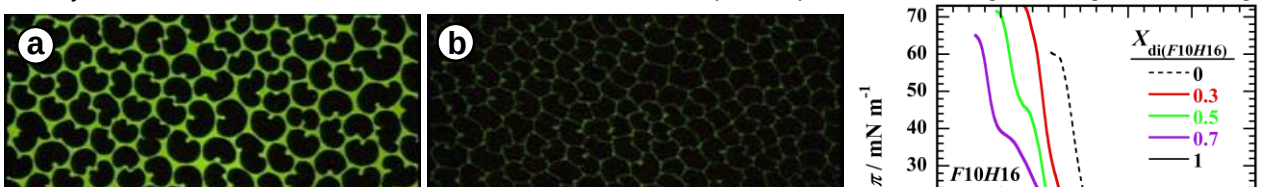

Figure 2. Fluorescence microscopy images of a,b) DPPC monolayers and c,d) binary DPPC/di(*F*10*H*16) monolayers ($X_{di(F10H16)}$ = 0.3) on water at a,c) 15 and b,d) 35 mN m^{-1}. The monolayers contained 1 mol% fluorescent probe NBD-PC. The scale bar represents 100 µm. e) *π*–*A* isotherms of DPPC, *F*10*H*16, di(*F*10*H*16) and mixed DPPC/di(*F*10*H*16) monolayers, and f) *π*–*A* and ∆*V*–*A* isotherms of the mixed monolayer at $X_{di(F10H16)}$ = 0.3 on water at 298.2 K.

isotherm compressions and fluorescence microscopy (FM) using a fluorescent probe (Figure 2). The domains of DPPC LC phase formed at the LE/LC phase transition are visible on the coexistence plateau (Figure 2a,d). They are dark and bean-shaped; the fluorescent probe is excluded from the LC phase but is soluble in the LE phase, which appears bright, while the LC phase is dark (Figure 2a). As surface pressure increases, the LC domains grow in number and become close-packed (Fig. 2b). Addition of di(*F*10*H*16) tetrablock totally changes the organization of DPPC when surface pressure reaches 12 mN m^{-1}. FM images display flower-like patterns tens of microns in size (Figure 2cd). These patterns consist of a central bright core, from which equally bright, elongated structures extend radially like bicycle spokes. The latter are ended by bright circular spots (~5-10 µm). The terminal spots exhibit a higher contrast than the DPPC LE phase regions, indicating that the FM probe is preferentially located inside these spots. Considering the probe's poor affinity with fluorocarbons, it is likely concentrated in a lipophilic neighborhood provided by the DPPC chains and the *H*16 segments of the tetrablocks. However, the bright spots are considerably larger than the di(*F*10*H*16) nanodomains, which cannot be observed by FM, whether in the presence or absence of the fluorescent probe. Essentially the same flower-like pattern is observed with Brewster Angle Microscopy (BAM, Supporting Information Figure S1), which proves that the arrangement is not induced by the fluorescent probe. Also of interest is that the terminal spots observed by BAM also display high contrast, revealing a local increase in height. These results indicate that the terminal spots likely consist of stacked aggregates of di(*F*10*H*16) nanodomains, as reported in the absence of phospholipids.[16]

Surface pressure (*π*)–molecular area (*A*) and surface potential (∆*V*)–*A* isotherms of mixed DPPC/di(*F*10*H*16) monolayers provide information on the organization of the molecules at the interface. The *π*–*A* isotherm of di(*F*10*H*16) is characterized by a sharp pressure rise for *A* smaller than 0.70 nm^2 (Figure 2e). The extrapolated area A_0 value of di(*F*10*H*16) is nearly twice (~0.65 nm^2) that of the *F*10*H*16 diblock (~0.35 nm^2, i.e., close to the cross-section of a perfluoroalkyl chain ~0.30 nm^2). Interestingly, the collapse pressure (π^c) decreases by dimerization (from 20 mN m^{-1} for *F*10*H*16 to 12 mN m^{-1} for di(*F*10*H*16); Fig. 2e), likely due to a lesser degree of freedom for di(*F*10*H*16) thermal motion during compression. Incorporation of di(*F*10*H*16) into DPPC monolayers at various molar fractions induces several breaks in the *π*–*A* isotherms. The LE/LC DPPC phase transition is still visible at ~12 mN m^{-1}, implying that DPPC and di(*F*10*H*16) are not miscible. In addition, the kinks kept apart, the shapes of *π*–*A* isotherms resemble more to that of DPPC than to that of di(*F*10*H*16), suggesting that DPPC is the major component present at the interface. Breaks are commonly considered to reflect 3D collapse or phase transitions. The *π*–*A* isotherms of the mixed monolayers are shifted to much smaller molecular area (*A)*, which indicates quantitative loss of di(*F*10*H*16) from the interface.

The ∆*V*-*A* isotherms of both *F*10*H*16 and di(*F*10*H*16) monolayers (Supporting Information Figure S2) decrease steadily upon compression and display negative values (−850 mV for di(*F*10*H*16), which indicates that the *F*10 segments are oriented toward air, while the *H*16 moieties are in contact with water. By contrast, ∆*V* of the DPPC monolayer increases upon compression, reaching +600 mV at maximal packing. The ∆*V*–*A* isotherms of the mixed monolayers show inflections that correspond to the breaks seen on the *π*–*A* isotherms. For all tetrablock molar fractions investigated, the ∆*V* variations observed around each inflection during compression are large in magnitude and, importantly, alternate negative and positive variations, reflecting

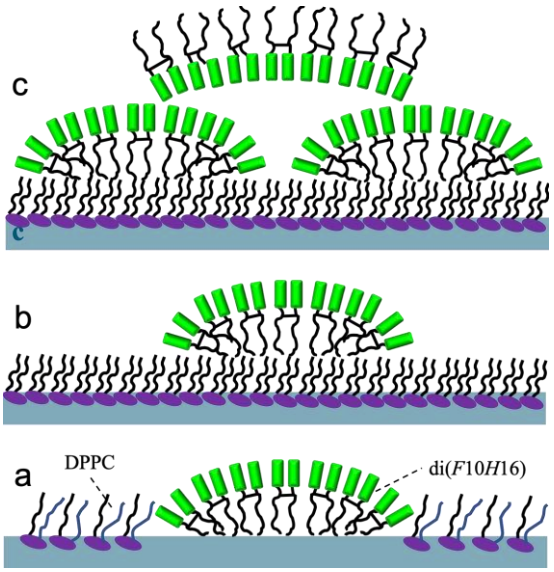

Scheme 1. Schematic representation of a) the coexistence of DPPC monolayer in LE phase and di(*F*10*H*16) tetrablocks forming surface nanodomains (*Fn* up and *Hm* down); b) ejection of nanodomains on top of the DPPC monolayer; **c)** formation of stacks of nanodomains and re-orientation of the diblocks with *Hm* up and *Fn* down.

opposite orientations, with either fluorinated or hydrogenated chains exposed to the air phase. In particular, for X = 0.3, the ΔV-A isotherm reveals thought-provoking features. Figure 2f shows that ΔV first increases, reflecting the increase in density of DPPC chains exposed to air. ΔV then reaches a plateau at A ~0.95 nm^2, indicating the coexistence of the DPPC LE phase with di(*F*10*H*16) nanodomains in contact with water (Scheme 1a). ΔV subsequently decreases sharply at A ~0.7 nm^2, which is ascribed to the ejection of the nanodomains on top of the DPPC monolayer (Scheme 1b), resulting in a vertical phase separation. It is expected that the tetrablocks are then oriented with their *Hm* segments in contact with the DPPC fatty chains and their *Fn* segments pointing towards air, as shown by SAXS for *F*8*H*16.[18] There is then a short plateau, followed by a further increase of ΔV (Scheme 1c, Figure 1f). This behavior signals a re-orientation of the tetrablock molecules, which appears concomitant with the LE/LC phase transition of the DPPC monolayer. A likely hypothesis is that the nanodomains form stacked layers in which the tetrablock molecules of the second layer are re-oriented and expose their *Hm* segments towards the air phase.

Next, Langmuir monolayers of DPPC/di(*F*10*H*16) mixtures were transferred onto mica substrates at 25 mN m^{-1}, using the Langmuir-Blodgett protocol, and investigated by atomic force microscopy (AFM). The binary DPPC/di(*F*10*H*16) films exhibit larger, flower-like structures that extend fingers outwards, and are comparable to those observed with FM and BAM (Figure 3A). These flower-like structures coexist with the di(*F*10*H*16) nanodomains that are no longer packed, but tend to align to form strings (Figure 3B). On the magnification (Figure 3C), it can be seen that the nanodomains (*a*) are excluded from the domains of LC phase (*b*, light brown) and are located preferentially on the LE phase regions of DPPC (*c*, dark brown). The difference in height between the DPPC LE phase region and the nanodomains is

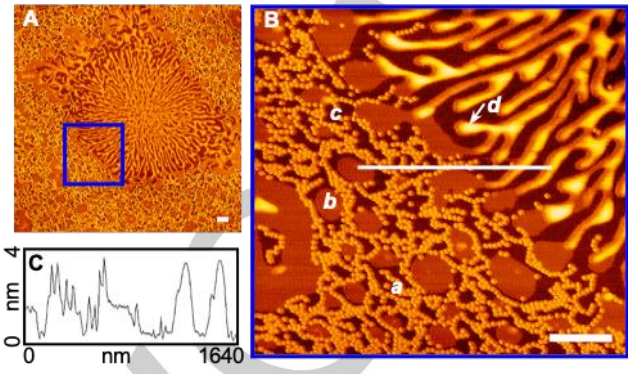

Figure 3. AFM topographic images of A) a binary DPPC/di(*F*10*H*16) monolayer (X = 0.3) transferred at 25 mN m^{-1} on mica; B) is an enlarged view of the area surrounded by a blue square in B showing the di(*F*10*H*16) nanodomains (*a*), DPPC LC (*b*) and LE (*c*) phases and the protruding fingers (*d*) of the flower-like structure shown in A. The scale bars represent 500 nm; The cross-sectional profile along the scanning line in B is provided in C

~1.2-1.8 nm (Figure 3C), suggesting that the disordered DPPC hydrocarbon chains are interleaved with tetrablock *H*16 chains. The fingers of the flower-like structure (bright domains *d*) have a height of ~3.6 nm, that is, are significantly higher that the DPPC LC phase, indicating that the nanodomains sit on top of the phospholipid phase.

These results indicate that the presence of di(*F*10*H*16) nanodomains dramatically perturbs the growth of the DPPC LC domains by concentrating at their boundaries. The growth of the DPPC LC domains is strongly intertwined with the gliding of the tetrablock nanodomains on top of the DPPC layer, which results in a decrease of the long-range dipole-dipole repulsions that exist among nanodomains. It is suggested that the nanodomains act as a 2D surfactant that adsorbs at the LE/LC boundary and decreases the line tension, leading to the formation of fingers. Such a 2D surfactant effect was seen with partially fluorinated compounds (called linactants) that lowered the line tension between fluorinated and hydrocarbon immiscible domains.[19] The shape of the DPPC LC domains was indeed found to change to complex branched morphologies by interaction with semifluorinated carboxylic acids and alcohols.[20] However, to our knowledge, such a drastic effect of nanometer-sized clusters have never been reported.

To sum up, we found that contact with organized self-assembled domains can profoundly modify the organization of monolayers of phospholipids. At the liquid expanded/liquid condensed phase transition of DPPC, di(*F*10*H*16) nanodomains form vertical stacks that glide on top of DPPC monolayers. Concurrently, the nanodomains profoundly change the morphology of the DPPC LC domains. As a result, the two compounds form novel, remarkable tens of micron-sized flower-like assemblies on the surface of water. These arrangements are preserved after transfer onto mica. In monolayers of di(*F*10*H*16), the monodisperse surface domains are close

packed even at zero pressure. However, in binary systems, the attractive force between the hydrocarbon segment of di(*F*10*H*16) and DPPC is likely to disturb the repulsive interaction and induce the formation of the large flower-like patterns.

The capacity for nanoscopic surface domains self-assembled from simple and nonpolar amphiphilic molecules to control 2D lipid organization and may provide an approach to fabrication of a organic templates. The specific 2D surfactant character of tetrablock nanodomains, and their possible solubilization properties, have potential for applications for clearance of hydrophobic substances from the air/solid and air/liquid interfaces. In particular, this ability could be used for pulmonary surfactant replacement therapy.[21] Vertical growth of hierarchical assembly of surface nanodomains with phospholipid monolayers may provide information on the stabilization of emulsions and vesicles, cell deformation mediated by endocytosis and exocytosis, and molecular recognition (at the level of lipid phase transitions) of cell membrane surfaces via signal transduction.

Experimental Section.

See the Supporting Information for the materials, experimental methods of π–*A* and ΔV–*A* isotherm measurements, and BAM, FM, and AFM observations.

Acknowledgements

This work was supported by a Grant-in-Aid for Scientific Research 16K08216 from the Japan Society for the Promotion of Science (JSPS).

Keywords: phospholipids • fluorinated alkanes • monolayers • self-assembled domains • nanodomain organization

[1] A. S. El-Tawargy, D. Stock, M. Gallei, W. A. Ramadan, M. A. S. El-Din, G. Reiter, R. Reiter, *Langmuir* **2018**, *34*, 3909−3917.
[2] L. Zhao, L. Zhiqun, *Soft Matter* **2011**, *7*, 10520-10535.
[3] M. F. Paige, A. F. Eftaiha, *Adv. Colloid Interface Sci.* **2017**, *248*, 129–146.
[4] G. v. Meer, D. R. Voelker, G. W. Feigenson, *Nat. Rev. Mol. Cell Biol.* **2008**, *9*, 112-124.
[5] H. M. McConnell, *Proc. Natl. Acad. Sci. USA* **1989**, *86*, 3452-3455.
[6] a) M. P. Krafft, *Acc. Chem. Res.* **2012**, *45*, 514-524; b) X.-H. Liu, J. G. Riess, M. P. Krafft, *Bull. Chem. Soc. Jpn. 90th Commemorative Account: Self-organization* **2018**, *91*, 846-857.
[7] a) M. Veschgini, W. Abuillan, S. Inoue, A. Yamamoto, S. Mielke, X.-H. Liu, O. Konovalov, M. P. Krafft, M. Tanaka, *ChemPhysChem* **2017**, *18*, 2791-2798; b) M. Veschgini, T. Habe, S. Mielke, S. Inoue, X.-H. Liu, M. P. Krafft, M. Tanaka, *Angew. Chem. Int. Ed.* **2017**, *56*, 12603–12607.
[8] a) J. Oelke, A. Pasc, A. Wixforth, O. Konovalov, M. Tanaka, *App. Phys. Lett.* **2008**, *93*, 213901; b) A. L. Simões Gamboa, E. Filipe, P. Brogueira, *Nano Lett.* **2002**, *2*, 1083-1086.
[9] M. Maaloum, P. Muller, M. P. Krafft, *Langmuir* **2004**, *20*, 2261-2264.
[10] a) J. Mackiewicz, B. Mühling, W. Hiebl, H. Meinert, N. Kociok, A. M. Joussen, *Graefes Arch. Clin. Exp. Ophthalmol.* **2008**, *246*, 69-79; b) P. Steven, A. J. Augustin, G. Geerling, T. Kaercher, F. Kretz, K. Kunert, J. Menzel-Severing, N. Schrage, W. Schrems, S. Krösser, M. Beckert, E. M. Messmer, *J. Ocul. Pharm. Ther.* **2017**, *33*, 678-685.
[11] J. G. Riess, *Chem. Rev.* **2001**, *101*, 2797-2920.
[12] C. Jacoby, S. Temme, F. Mayenfels, N. Benoit, M. P. Krafft, R. Schubert, J. Schrader, U. Flögel, *NMR Biomed.* **2014**, *27*, 261–271.
[13] a) F. Haiss, R. Jolivet, M. T. Wyss, J. Reichold, N. B. Braham, F. Scheffold, M. P. Krafft, B. Weber, *J. Physiol.* **2009**, *587*, 3153-3158; b) R. Dembinski, R. Bensberg, G. Marx, R. Rossaint, M. Quintel, R. Kuhlen, *Exp. Lung. Res.* **2010**, *36*, 499-507.
[14] M. P. Krafft, *Biochimie* **2012**, *94*, 11-25.
[15] A. Wójcik, P. Perczyk, P. Wydro, M. Broniatowski, *BBA Biomembranes* **2018**, *1860*, 2576–2587.
[16] C. de Gracia Lux, J.-L. Galliani, G. Waton, M. P. Krafft, *ChemPhysChem* **2012**, *13*, 1454-1462.
[17] H. Nakahara, S. Lee, O. Shibata, *Biophys. J.* **2009**, *96*, 1415-1429.
[18] P. Fontaine, M. Goldmann, P. Muller, M.-C. Fauré, O. Konovalov, M. P. Krafft, *J. Am. Chem. Soc.* **2005**, *127*, 512-513.
[19] S. Trabelsi, S. Zhang, R. Lee, D. K. Schwartz, *Phys. Rev. Lett.* **2008**, *100*, 037802.
[20] A. Eftaiha, S. M. K. Brunet, M. F. Paige, *Langmuir* **2012**, *28*, 15150-15159.
[21] a) H. Nakahara, S. Lee, M. P. Krafft, O. Shibata, *Langmuir* **2010**, *26*, 18256-18265; b) H. Nakahara, M. P. Krafft, A. Shibata, O. Shibata, *Soft Matter* **2011**, *7*, 7325-7333.